

Ignition–extinction of ethane–air mixtures over noble metals

M. Ziauddin, G. Vesper^{*,‡} and L.D. Schmidt[‡]

Department of Chemical Engineering and Materials Science, University of Minnesota, Minneapolis, MN 55455, USA

Received 20 December 1996; accepted 17 April 1997

Surface ignition–extinction, homogeneous ignition and autothermal behavior of ethane–air mixtures are examined over Pt, Pd, Rh, Ir and Ni foils for the full range of fuel–air ratios. The observed trends are explained in terms of metal–oxygen bond strengths and reaction pathways catalyzed by these metals.

Keywords: ignition–extinction, hydrocarbon oxidation/combustion near surfaces, ethane oxidation, noble metal catalysis, platinum catalyst, palladium catalyst, rhodium catalyst, iridium catalyst, nickel catalyst

1. Introduction

Catalytic oxidation of alkanes is important in a wide variety of industrial processes ranging from catalytic incineration for fuel-lean feeds, to catalytic combustion near stoichiometric fuel feeds, and catalytic partial oxidation for fuel-rich feeds [1–4]. For the design and safe operation of these processes a precise knowledge of heterogeneous ignition–extinction temperatures as well as homogeneous ignition temperatures near the catalyst surface, is of prime importance. In this study we examine these variables for five industrially important catalysts and investigate the trends observed for ethane oxidation in these systems.

In a recent study we examined ignition–extinction behavior of various hydrocarbons over Pt foils [5]. We observed a common trend in the oxidation of alkanes (methane, ethane, propane and isobutane) and a different trend for alkenes (ethylene and propylene). In the case of alkanes it was found that the surface was poisoned by oxygen prior to heterogeneous ignition, and therefore ignition temperature generally decreased as the fuel concentration in the feed was increased. In the case of alkene oxidation, the surface was mostly covered by hydrocarbon fragments prior to ignition, and therefore the surface ignition temperatures generally increased with increase in feed fuel concentration. In the present study we compare the oxidation of a single alkane, ethane, over various metals, Pd, Rh, Ir and Ni. Previous results on Pt are included for comparison.

The metals investigated in this study are not as “noble” as Pt, and under reaction conditions they can form more or less stable compounds and overlayers with oxygen and carbon which alter their activity. Therefore, unlike Pt, the ignition–extinction behavior over these

metals depends more strongly on the reaction conditions under which it was operated previously. For example, the oxides of these metals alter the activity significantly and the results are dependent on whether the catalyst was previously operated under oxidizing (excess air) or reducing (excess fuel) conditions. Due to their greater interactions with reactants, these metals display a far more complex behavior than Pt. Hysteresis in activity and oxygen content is well established at least on Pd catalysts [6], and oscillations in activity of Ni foils, due to successive oxidation and reduction of the foil, have been observed [7]. Consequently, studies of these metals are more difficult and therefore less numerous than those on Pt catalysts [8–13].

There are a few comparative studies of hydrocarbon oxidation over metal catalysts in the literature, however, none of them investigates the ignition–extinction behavior of these reactions [14–17]. Huff et al. and Tornianinen et al. have done comparative studies on these metals under nearly adiabatic conditions [14,15]. Selectivities to partial oxidation products over several metal-coated monolith foams were investigated at very short contact times and the dominant reactions pathways over these catalysts were identified. However, they only investigated autothermal operation in excess fuel and ignition–extinction temperatures were not examined quantitatively. Firth and Holland investigated complete methane oxidation in excess oxygen on several supported noble metals [16] and Coward and Guest made a comparative study on homogeneous ignition of stagnant natural gas–air mixtures over several metals many years ago [17]. However, neither group examined the surface ignition–extinction behavior for these catalysts.

There are several other studies on each of these metals individually in the literature, but the reaction conditions for these are so different that a comparison of these metals on an equivalent basis is not possible. Moreover, most of the studies have been on supported metal sys-

* Present address: ICVT, Universität Stuttgart, 70199 Stuttgart, Germany.

‡ To whom correspondence should be addressed.

tems, so that the complex interaction of the metal with the support has to be accounted for. For example, investigations on Pd have been mostly on alumina supports, and there is a considerable disagreement in the literature about the change in activity at high temperatures [6,18–24]. The change in activity has been attributed to the $\text{Pd} \leftrightarrow \text{PdO}_x$ transformation, Pd–support interaction, sintering etc. As the present study is on high-purity polycrystalline metal foils, problems due to sintering and metal–support interaction are completely avoided and thus, the results are representative of the intrinsic metal property.

In this study we compare five metals in a single, simple, well defined experimental setup, which produces reproducible data with small experimental scatter. All metals are compared on an equivalent basis and the entire feed composition range is investigated. This study of a single hydrocarbon over different metals in conjunction with our previous study of different hydrocarbons over a single metal allows us to assemble a more complete picture of alkane oxidation.

2. Experimental apparatus and procedure

The experimental procedure used in this study was described in detail earlier [5]. The experiments were conducted in a quartz tube reactor with a diameter of 3 cm as shown in figure 1a. Reactant gases, ultra-high-purity air and CP grade ethane, were mixed in a glass tube filled with glass beads and then introduced into the reactor. A high-purity metal foil ($> 99.5\%$, Johnson Matthey) was cut to approximate dimensions of $20 \times 3 \times 0.025 \text{ mm}^3$ and placed perpendicular to the gas flow in a stagnation flow configuration. The foil was heated resistively by a variable current power supply. The current output from the power supply and the voltage drop across the foil were recorded to determine the power input to the foil. The foil temperature was measured by a chromel/alumel thermocouple spot-welded to the foil.

In all experiments except those at very fuel-rich feeds, the air flow rate was kept constant at 3 slpm (standard liters per minute), and the ethane flow rate was changed to change the fuel–air ratio. For very fuel-rich feeds that

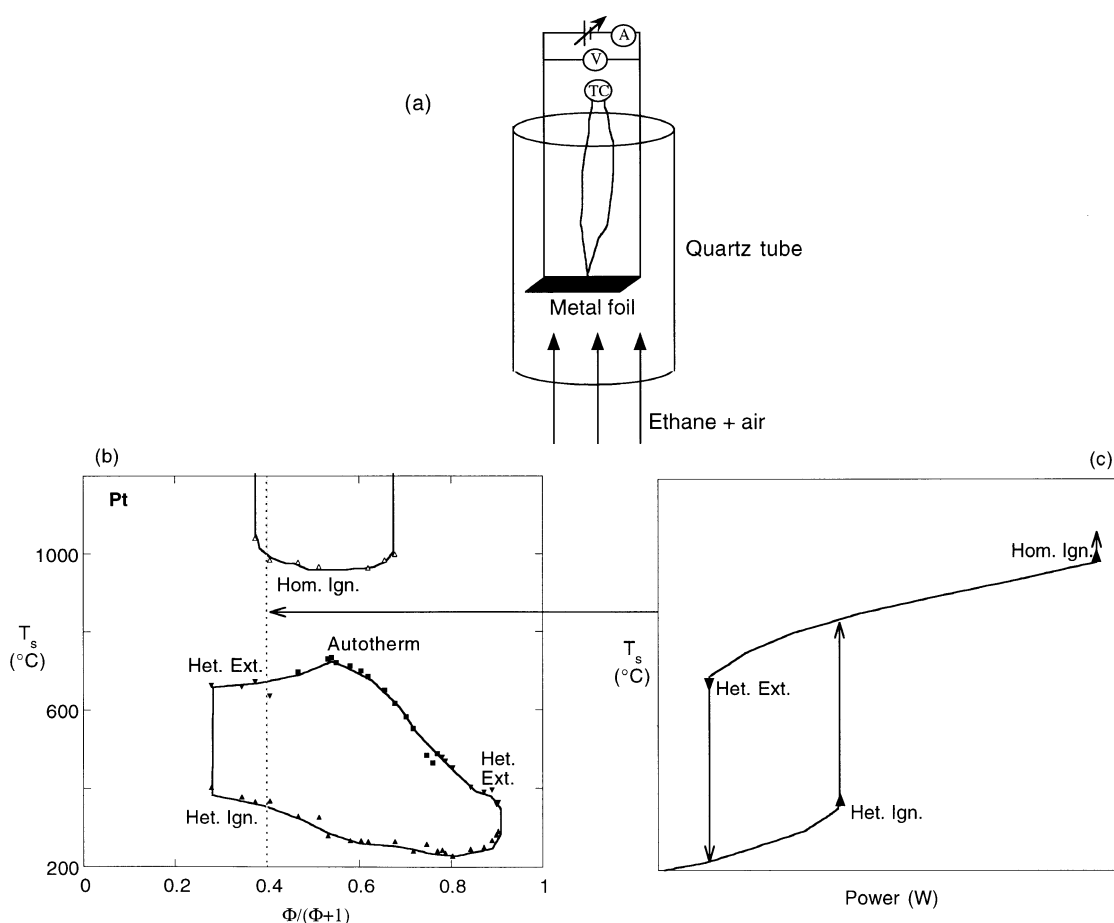


Figure 1. (a) Experimental apparatus, (b) a typical two-parameter bifurcation plot and (c) a typical surface temperature (T_s) vs. electrical power plot (P_w). T_s vs. P_w plots like (c) were obtained at several fuel compositions and heterogeneous ignition–extinction, autothermal temperatures and homogeneous ignition temperatures were read from these curves and compiled in a two-parameter bifurcation plot.

required ethane flow rates greater than 2 slpm, the air flow rate was reduced so that the total flow rate (air + ethane) was between 3 and 5 slpm. Varying the total flow rate between 3 and 5 slpm (velocity of 10–17 cm/s) did not affect the results significantly. Reynolds number based on entrance conditions and tube diameter ranged from 150 to 250. Before taking any data, all foils were heated in air to about 1100°C for 30–60 min and then aged under reaction conditions for at least 2–3 h. However, for Rh foils much longer aging times (~ 24 h) were necessary before completely reproducible data could be obtained. Foils that deactivated due to oxide formation were reduced either with 10% H_2 in Ar mixture or by operation in excess fuel for several hours to restore activity. Foils that deactivated due to coke formation were heated in air at temperatures above 1000°C to reactivate.

Ignition–extinction temperatures were determined from turning points on the steady state surface temperature (T_S) vs. electrical power (P_W) plot. A data point (T_S , P_W) was considered stationary if the mean values of both T_S and P_W over a period of 10 s did not vary by more than twice the noise level over a period of 1 min. A typical steady state T_S vs. P_W plot at a fixed fuel–air ratio is shown in figure 1c and the heterogeneous ignition–extinction and homogeneous ignition temperatures are marked. In cases where the surface reaction remained ignited at zero power input, the foil temperature at zero power was taken as the autothermal temperature. For Ni, autothermal operation was not observed, but oscillations at a constant current input were seen above a certain base temperature. In this case, the base temperature at which oscillations (period < 10 min) started was taken as the ignition temperature.

These T_S vs. P_W curves were obtained at various fuel–air ratios, and the ignition–extinction data was compiled in a two-parameter bifurcation plot, as shown in figure 1b. In this figure, ignition–extinction temperatures are plotted against the feed composition. Instead of the usual equivalence ratio ($\Phi = (\text{fuel}/\text{air})/(\text{fuel}/\text{air})_{\text{stoich}}$), the modified equivalence ratio ($\Phi/(1 + \Phi)$) is used to depict the feed composition so that fuel-rich and fuel-lean compositions can be shown together. The modified equivalence ratio maps the entire range of feed compositions on scale of 0 to 1 instead of 0 to infinity, and thus, puts equal weight on the fuel-lean and fuel-rich sides of the diagram with $\Phi/(1 + \Phi) = 0.5$ corresponding to the $CO_2 + H_2O$ stoichiometry.

All data points, except surface ignitions on Rh, Ir and Ni, were reproducible to within ± 10 K on the same foil and ± 15 K on different foils. Surface ignitions on Rh, Ir and Ni were only reproducible to ± 20 K on the same foil and ± 40 K on different foils, probably because the foils were oxidized to varying degrees as they were heated to ignition temperatures. The data was reproduced on at least five foils for each metal.

3. Results

3.1. Platinum

The results on Pt have been reported earlier [5]. The two-parameter (temperature and composition) bifurcation diagram obtained from several S curves is shown in figure 1b. The most remarkable feature of the result is that Pt shows stable operation in both excess air and excess fuel, and shows no deactivation either due to coke or oxide formation. Also note that except for very rich feeds the surface ignition temperatures drop continuously as the fuel concentration in the feed is increased.

3.2. Palladium

The two-parameter bifurcation diagram for Pd is shown in figure 2a. The figure shows that the heterogeneous ignition temperatures remain fairly constant for the entire composition range and only a slight increase in ignition temperatures is seen in very lean fuel mixtures. The S curves in region A, B and C exhibited qualitatively different behavior and are shown in figures 3a–3c. Note the two distinct curvatures for the autothermal curve (figure 2a) and the increased foil activity in region B above 800°C (figure 3b). No significant change in activity was seen for leaner mixtures (region A) at similar temperatures. The shaded region in figure 2a indicates deactivation due to coking. In this region an active Pd foil ignited at the indicated temperature but deactivated after about 1–30 min of operation. Coke was then visually observed on the deactivated catalyst.

XPS was performed on the Pd foils after surface and homogeneous ignition. The surface consisted mostly of PdO_x before heterogeneous ignition and mostly of Pd metal at homogeneous ignition temperatures.

3.3. Rhodium

The two-parameter bifurcation diagram for Rh is shown in figure 2b. The shaded area indicates deactivation. When an active foil was heated rapidly in this region, it ignited at about 500–600°C, but deactivated after about 30–60 min of operation at temperatures of about 700–800°C. The deactivated foil no longer showed ignitions in the 500–600°C temperature range. (This behavior is similar to Ir and is discussed with a T_S vs. P_W graph below.) However, when the deactivated foil was heated to about 1000°C heterogeneous ignition was again observed (figure 3d). Long-term operation (> 5 h) in this ignited state above a 1000°C was not possible because of metal loss due to oxide evaporation. Note from figure 3d that Rh displays a much higher activity on cooling than on heating. No hysteresis was seen if the deactivated foil was heated to temperatures below 900°C and then cooled.

In region B, Rh showed no deactivation over a period

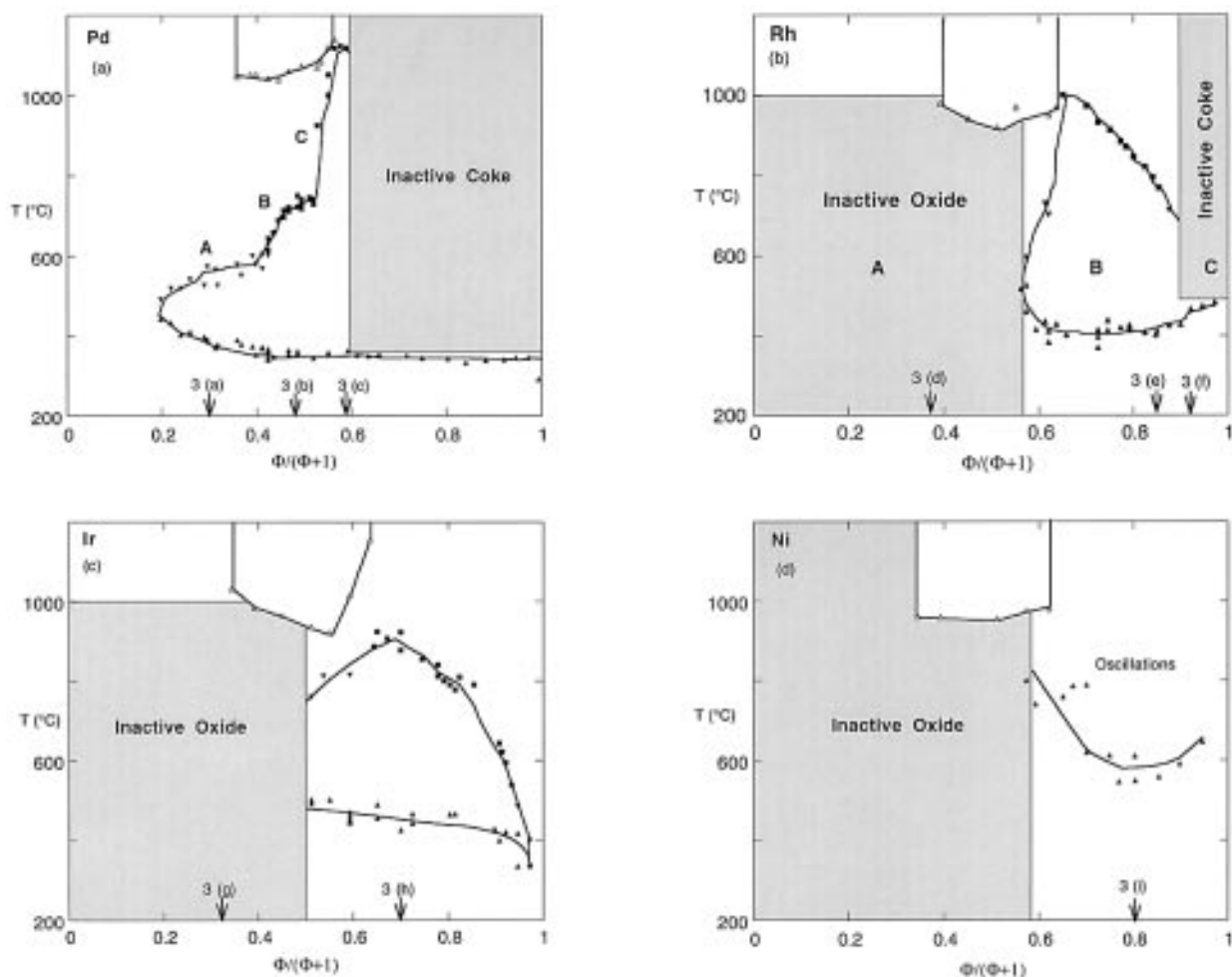


Figure 2. Two-parameter bifurcation plots for Pd (a), Rh (b), Ir (c) and Ni (d). (▲) depict surface ignition temperatures, (▼) depict surface extinction temperatures, (■) depict autothermal temperatures and (△) depict homogeneous ignition temperatures. T_S vs. P_W plots at the indicated compositions are shown in figure 3.

of several hours. A typical S curve in this region is shown in figure 3e. Note from figure 2b that the homogeneous ignition temperatures and the autothermal curve are close to each other. The autothermal curve in this region was obtained by starting with a feed richer in fuel than the homogeneous flammability limit and then slowly decreasing the fuel concentration. Homogeneous ignition temperatures were obtained in the usual way i.e. by heating the foil at a fixed fuel–air ratio until the gas phase ignited.

In region C, Rh deactivated and a typical S curve is shown in figure 3f. The total time on the ignited branch was 25 min. No visual coke was seen on the deactivated foil.

3.4. Iridium

The two-parameter bifurcation diagram for Ir is shown in figure 2c and the T_S vs. P_W plots are shown in figures 3g–3h. The shaded region in figure 2c indicates deactivation. In the shaded region an active Ir foil, which was previously operated in excess fuel for several hours,

deactivated when operated in excess air, as shown in figure 3g. In this figure, the arrows indicate heating or cooling. The time spent on the heating branch is about 35 min, which includes at 15 min period in which the temperature was kept constant at 740°C. Note that the power required to maintain the foil at 740°C increases as the foil deactivates. On cooling Ir shows no activity, which is indicated by an almost linear dependence of T_S on P_W . Also note that for the same power input a higher temperature is observed on the heating branch than on the cooling branch. Like Rh, catalytic activity on a deactivated Ir foil was recovered at temperatures above 1000°C and the S curves for Ir in this case are similar to those of Rh (figure 3d).

Figure 3g shows a typical S curve for Ir in excess fuel. No deactivation was observed under these conditions over a period of several hours.

3.5. Nickel

The two-parameter bifurcation diagram for Ni is shown in figure 2d. No autothermal behavior was

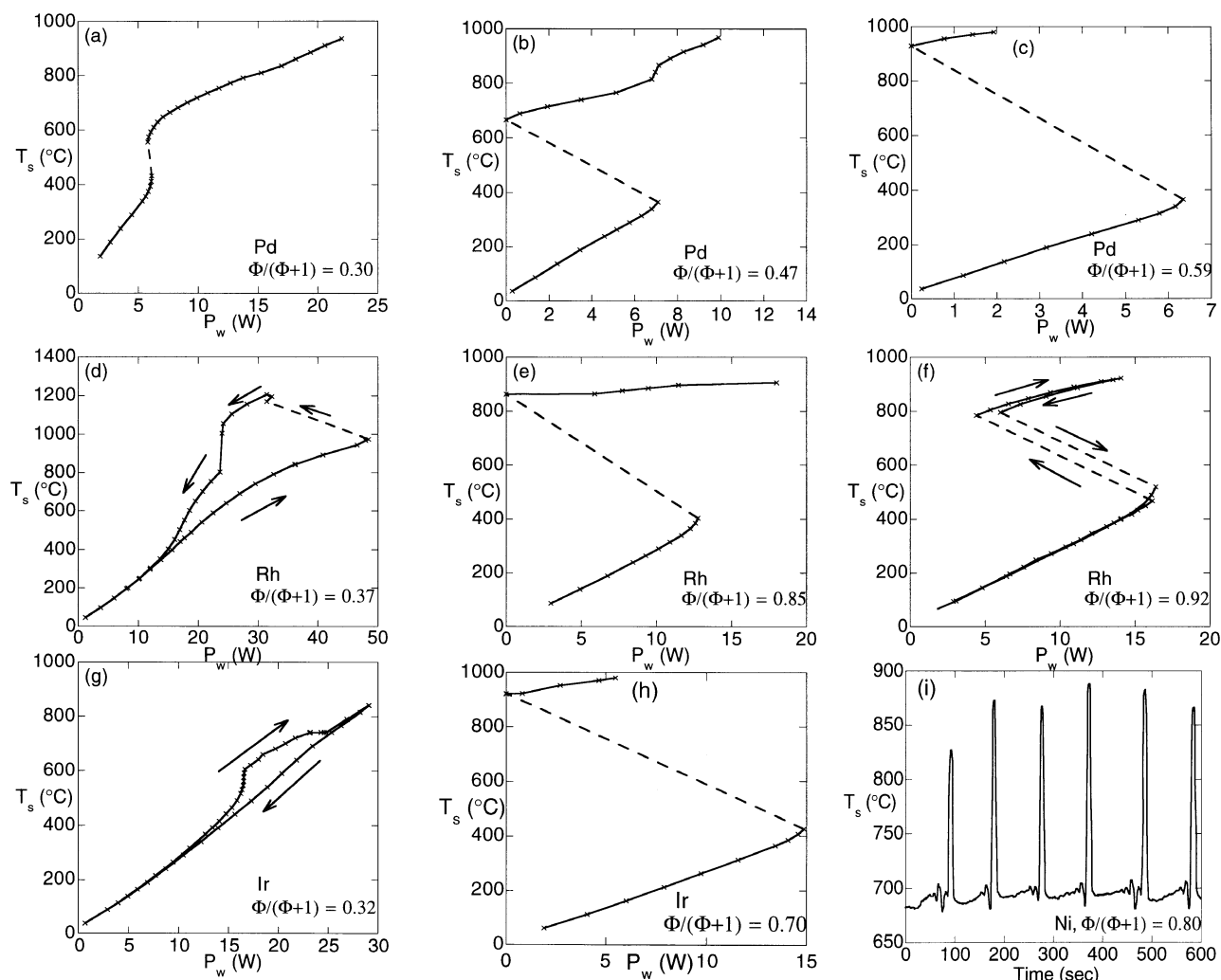


Figure 3. Surface temperature (T_s) vs. electrical power (P_w) plots for Pd (a)–(c), Rh (d)–(f) and Ir (g)–(h), and surface temperature trace for Ni (i).

observed on Ni under any feed composition, and it deactivated rapidly in excess air. In the fuel-rich region, oscillations at constant current input were observed at temperatures above $\sim 600^\circ\text{C}$, and a sample is shown in figure 3i. The period, amplitude and the shape of the oscillations changed with the feed composition and the base temperature.

4. Discussion

In the presented experiments we have investigated the oxidation of ethane over five industrially important metal catalysts. It is surprising to find that these “noble” metals with many common physical and chemical properties show such large differences in their catalytic activity. The complete bifurcation diagrams (figures 1 and 2) reported here clearly mark the limits of operation for these catalysts and at the same time yield insight into the catalytic chemistry. These diagrams help identify poten-

tial catalysts for partial oxidation and lean combustion applications. Both practical and scientific implications of these bifurcation maps are discussed in the following sections. Simple explanations for trends observed in ignition temperatures and catalyst deactivation are provided.

4.1. Surface ignition

Figure 4a shows that Pd, Rh and Ir are ignitable in much more fuel-rich feeds than Pt, and ignition temperatures are generally in the order $\text{Pt} < \text{Pd} < \text{Rh} < \text{Ir} < \text{Ni}$. Pt has the widest ignition–extinction region and does not deactivate in either excess air or fuel. Pd is the only other metal that is active in excess air; although it deactivates rapidly in excess fuel (figure 2a). Rh, Ir and Ni show activity in excess fuel only, and deactivate rapidly in excess air (figures 2b–2c).

In an earlier study we presented a simple model for alkane oxidation on Pt [5]. The model was based on a

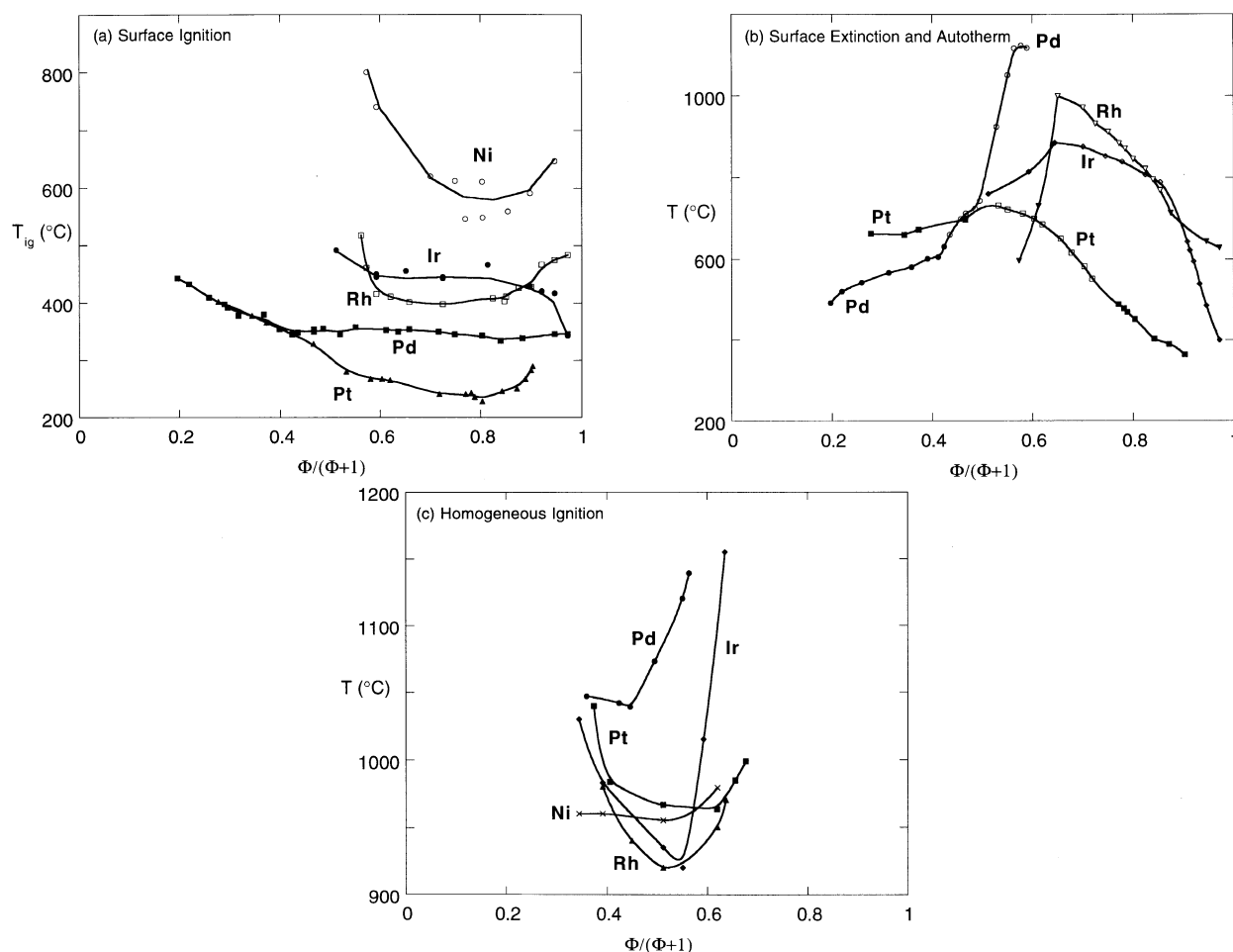


Figure 4. Surface ignition temperatures (a), extinction (filled symbols) and autothermal (unfilled symbols) temperatures (b), and homogeneous ignition temperatures (c) for Pt, Pd, Rh, Ir and Ni.

Langmuir–Hinshelwood mechanism with competitive adsorption of the reactant gases and predicted catalytic ignition temperatures well. The model was thus able to show that surface ignition was mainly controlled by desorption of oxygen, which blocks the surface before ignition. These model results extend well to the present study.

The oxide stability and the M–O bond strength are generally in the order $\text{Pt} < \text{Pd} < \text{Rh} < \text{Ir} < \text{Ni}$ [25], and the ignition temperature and composition correlate well with these. Pt and Pd with the lowest M–O bond strength have the lowest ignition temperatures and are active in the leanest fuel mixtures. The strong interaction of Rh, Ir and Ni with oxygen deactivates these metals in the fuel-lean region (oxidizing environment) and ignitions are only seen after the oxide decomposes or evaporates. In excess fuel Rh and Ir do not deactivate, most likely due to a net reducing environment which prevents the formation of a stable oxide. Ni with the highest M–O bond strength forms an oxide even in excess fuel, and shows oscillatory behavior due to successive oxidation and reduction of the surface. The probable mechanism of the oscillations is based on a lower catalytic activity of

the oxidized surface versus the reduced surface. At low temperatures in the cycle the surface is preferentially reduced and the activity increases which results in a rise in the surface temperature. However, as the surface temperature rises surface oxidation becomes more favorable and the activity and the surface temperature once again drop. This oxidation–reduction mechanism for Ni has been suggested previously [7,26,27].

Thus, we generally see that with an increase in the M–O bond strength both the temperature and the fuel content of the feed required for ignition increase. Figure 5a shows a plot of T_{ig} vs. metal–oxygen binding energy (BE, from TPD) [25,28]. Ignition temperatures were taken at $\Phi/(1 + \Phi) = 0.6$ as all metals exhibited stable operation at this feed composition. The figure shows an almost linear dependence of ignition temperatures on the M–O bond strength, except for Ni which forms a stable oxide.

It is interesting to note that ignition temperatures for Pt generally drop with the fuel feed composition, while for Pd they are almost independent of the feed composition. This result is consistent with the picture of oxygen desorption controlling ignition as presented above.

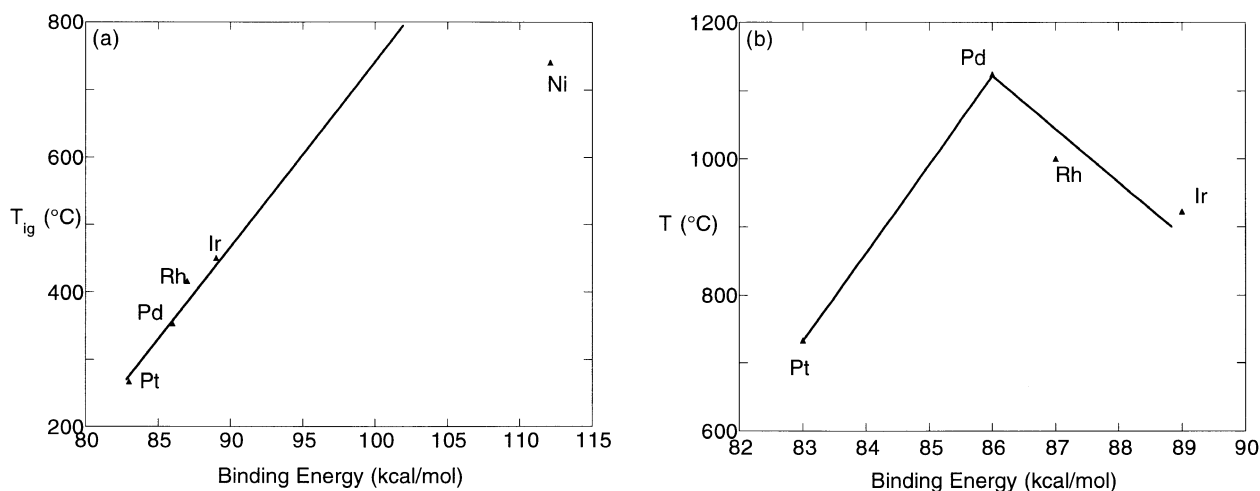


Figure 5. (a) Ignition temperatures (at $\Phi/(1 + \Phi) = 0.6$) plotted against the metal–oxygen binding energy from TPD experiments. (b) The highest autothermal temperature observed for the indicated metal is plotted against the metal–oxygen binding energy.

Since the Pt–O bond is fairly weak, oxygen poisoning is reduced as the fuel–air ratio increases. However for Pd, the Pd–O bond is sufficiently strong, and oxygen desorption probably remains the rate limiting step, even in excess fuel.

The ignition curve for Rh is nearly flat while for Ir it seems to have a slightly negative slope and for Ni it shows a minimum. However, since these trends lie within the experimental error bounds for these metals no definite conclusions from these differences should be drawn. As noted previously, the scatter in data is probably because the foils were oxidized to different degrees as they were heated to ignition temperatures.

4.2. Surface extinction and autotherms

Figure 4b shows the surface extinction (filled symbols) and autothermal temperatures (unfilled symbols) for metals investigated in this study. Only a few data points are included for each metal to show the curves. Once again note that Pt shows stable operation in both excess air and excess fuel. Pd is active in excess air but deactivates in excess fuel. Rh and Ir deactivate in excess air but show stable operation in excess fuel. These results are consistent with the correlation between the activity and the M–O bond strength presented above.

It is interesting to note that Pd shows two distinct autotherms. The composition range for the first autotherm is $0.42 < \Phi/(1 + \Phi) < 0.50$ and the temperature range is 630–740°C, and the composition range for the second autotherm is $0.50 < \Phi/(1 + \Phi) < 0.60$ and the temperature range is 740–1120°C. Also note that the S-curve for Pd at $\Phi/(1 + \Phi) = 0.47$ (figure 3b) shows increased activity above the composition temperatures of PdO ($\sim 800^\circ\text{C}$). These results strongly suggest that the first autotherm is on an oxide surface, while the second autotherm is on metallic Pd. The increase in activity observed at temperatures above 800°C (figure 3b) is

most likely due to the exposure of a more metallic surface after decomposition of the oxide, and it is possible that this increased activity develops into the higher autotherm observed at more fuel-rich feeds. These results imply that in excess air and at temperatures below 800°C PdO_x is the active phase, while in excess fuel and at temperatures above 800°C Pd metal is active.

It is remarkable that PdO_x is active, while oxides of Rh, Ir and Ni completely deactivate the catalyst. However, the behavior of PdO_x is consistent with the correlation between M–O bond strength and activity presented above. The Pd–O bond strength is intermediate between that of Pt–O and Rh–O, and maybe it is just the right strength for PdO_x to be active. The Pt–O bond may be too weak, while the Rh–O bond may be too strong for PtO_x and RhO_x to be active. The same trend is seen in the peak autothermal temperatures observed over these metals (figure 5c). The plot is reminiscent of a volcano type relationship. However, it differs from a true volcano plot because autothermal temperatures are a function of both the reaction rate and the selectivity.

A further explanation for the difference in autothermal temperatures over these metals lies in the different reaction pathways catalyzed by these metals. Huff et al. have identified the major reaction products in ethane oxidation over Pt, Pd and Rh, on metal-coated monoliths in excess fuel [29]. On Pt, the main reaction product was C₂H₄ (70% selectivity, 80% conversion). On Rh, syngas (CO + H₂) production dominated ($\sim 70\%$ selectivity, 95% conversion), while on Pd no stable operation was possible due to heavy carbon deposition. Torniainen et al. have investigated methane oxidation over several metals, with an experimental setup similar to that of Huff et al. [15]. They observed that Ir had an activity intermediate between Pt and Rh. These results suggest that the autothermal temperatures on Pt are much lower than that on Ir or Rh, due to the fact that Pt favors the

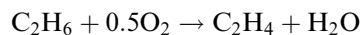
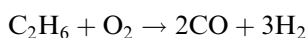
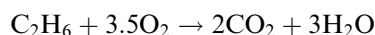
less exothermic reaction of C_2H_4 formation, while Ir and Rh favor the more exothermic syngas production.

4.3. Homogeneous ignitions

Figure 4c shows the homogeneous ignition temperatures for all metals investigated in this study. Only a few data points are shown for each metal. Note that, compared to other metals, homogeneous ignition temperatures on Pd are considerably higher. The upper flammability limits in the order of increasing $\Phi/(1 + \Phi)$ are Pd (0.56), Ni (0.62), Rh (0.64), Ir (0.64) and Pt (0.68), while the lower flammability limit is at about 0.35 for all metals investigated.

Linan and Williams have suggested that a sufficiently fast surface reaction can delay homogeneous ignition by depleting the reactants from the boundary layer [30]. This depletion of the boundary layer makes a lean gas mixture leaner and a rich gas mixture richer, and thus may move the composition in the boundary layer of the flammability limit [31]. Therefore, the flammability limits of combustible gases near a catalytic surface are narrower than the usually determined flammability limits. Homogeneous ignitions on Pd agree well with this hypothesis. Pd has the highest autothermal temperatures, and thus probably it is the most efficient catalyst in depleting the boundary layer of reactants and suppressing homogeneous ignition.

In contrast to the above, it is surprising that the lower flammability limit agrees closely for all metals investigated. A possible explanation for this behavior could be based on the different reaction selectivities in the fuel-rich regime over the different catalysts. Obviously, several different products are possible for partial oxidation reactions, while total oxidation only yields CO_2 and H_2O . Thus, different metals will catalyze different reaction pathways under fuel-rich conditions (e.g., Pt catalyzes oxidative dehydrogenation, while Rh, Ir, Ni favor syngas production). Due to correspondingly different reaction stoichiometries, they will thus differ in their ability to deplete the boundary layer of O_2 , the limiting reactant under these conditions:



Under fuel-lean conditions on the other hand, complete oxidation will dominate the reaction over any catalyst. Thus the boundary layer will be depleted equally and all metals will show similar lower flammability limits.

5. Summary

In this study we have determined complete bifurcation

diagrams for the oxidation of ethane over Pd, Rh, Ir and Ni. This study was a direct extension of our earlier work in which we examined the oxidation of several hydrocarbons on a Pt surface [5]. Ongoing research in our lab investigates the oxidation of methane near Pd, Rh, Ir and Ni surfaces. The intent of these investigations is to obtain consistent bifurcation data for hydrocarbon oxidation over noble metal catalysts.

In the oxidation of ethane, Pt showed stable operation without any deactivation in either excess air or fuel. All other noble metals deactivated either due to the formation of oxides in excess air (Rh, Ir, Ni) or due to coke formation in excess fuel (Pd, Rh). Heterogeneous ignition temperatures were generally in the order $Pt < Pd < Rh < Ir < Ni$. The results correlated well with the M–O bond strength. Pt and Pd with the lowest M–O bond strength had the lowest ignition temperatures and ignited in the leanest fuel mixtures, while Rh, Ir and Ni with high M–O bond strengths, had high ignition and deactivated in excess air. Rh and Ir showed stable operation in excess fuel, possibly because the oxides were not stable in the net reducing environment. Finally, Ni with the highest M–O bond strength showed oscillatory behavior in excess fuel due to successive oxidation and reduction of the surface.

Acknowledgement

This research was supported by DOE under grant DE-FG02-88ER13878-A02. Financial support by the A. v. Humboldt-foundation and the DFG through fellowships to GV are gratefully acknowledged.

References

- [1] L.D. Pfefferle and W.C. Pfefferle, *Catal. Rev. Sci. Eng.* 29 (1987) 219.
- [2] W.C. Pfefferle and L.C. Pfefferle, *Progr. Energy Combust. Sci.* 12 (1986) 25.
- [3] R. Prasad, L.A. Kennedy and E. Ruckenstein, *Catal. Rev. Sci. Eng.* 26 (1984) 1.
- [4] L.D. Schmidt and M. Huff, *Catal. Today* 21 (1994) 443.
- [5] G. Veser and L.D. Schmidt, *AIChE J.* 42 (1996) 1077.
- [6] P. Salomonsson, S. Johansson and B. Kasemo, *Catal. Lett.* 33 (1995) 1.
- [7] L. Lobban and D. Luss, *J. Phys. Chem.* 93 (1989) 6530.
- [8] A. Balakrishna, L.D. Schmidt and R. Aris, *Chem. Eng. Sci.* 49 (1994) 11.
- [9] R.J. Olsen et al., *Chem. Eng. Sci.* 47 (1992) 2505.
- [10] X. Song, W.R. Williams, L.D. Schmidt and R. Aris, *Combust. Flame* 84 (1991) 292.
- [11] X. Song, L.D. Schmidt and R. Aris, *Chem. Eng. Sci.* 46 (1991) 1203.
- [12] W.R. Williams et al., *Combust. Flame* 84 (1991) 277.
- [13] W.R. Williams, J. Zhao and L.D. Schmidt, *AIChE J.* 37 (1991) 641.
- [14] M. Huff, P.M. Torniainen and L.D. Schmidt, *Catal. Today* 21 (1994) 113.

- [15] P.M. Torniainen, X. Chu and L.D. Schmidt, *J. Catal.* 146 (1994) 1.
- [16] J.G. Firth and H.B. Holland, *Trans. Faraday Soc.* 65 (1969) 1121.
- [17] H.F. Coward and P.G. Guest, *J. Am. Chem. Soc.* 49 (1927) 2479.
- [18] J.G. McCarty, *Catal. Today* 26 (1995) 283.
- [19] F.H. Riberio, M. Chow and R.A. Dalla Betta, *J. Catal.* 146 (1994) 537.
- [20] N. Mouaddib et al., *Appl. Catal. A* 87 (1992) 129.
- [21] A.K. Bhattacharya et al., *Appl. Catal. A* 80 (1992) L1–L5.
- [22] P. Briot and M. Primet, *Appl. Catal.* 68 (1991) 301.
- [23] R.J. Farrauto et al., *Appl. Catal. A* 81 (1992) 227.
- [24] T.R. Baldwin and R. Burch, *Appl. Catal.* 66 (1990) 337.
- [25] R.J. Madix and J.T. Roberts, *Surface Reactions*, ed. R.J. Madix (Springer, Berlin) pp. 5–53.
- [26] Z. Kurtanek, M. Sheintuch and D. Luss, *J. Catal.* 66 (1980) 11.
- [27] T. Lindstrom and T. Tsotsis, *Surf. Sci.* 150 (1985) 487.
- [28] J.B. Benziger and R.E. Preston, *Surf. Sci.* 141 (1984) 567.
- [29] M. Huff and L.D. Schmidt, *Catal. Today* 21 (1994) 443.
- [30] A. Linan and F.A. Williams, *SIAM J. Appl. Math.* 40 (1981) 261.
- [31] C.K. Law and S.H. Chung, *Combust. Sci. Technol.* 32 (1983) 307.